

Intrinsic nonlinearity of the light–current characteristic of semiconductor lasers with a quantum-confined active region

Levon V. Asryan^{a)}

State University of New York at Stony Brook, Stony Brook, New York 11794-2350 and Ioffe Physico-Technical Institute, St Petersburg 194021, Russia

Serge Luryi^{b)}

State University of New York at Stony Brook, Stony Brook, New York 11794-2350

Robert A. Suris^{c)}

Ioffe Physico-Technical Institute, St Petersburg 194021, Russia

(Received 23 April 2002; accepted for publication 27 July 2002)

We describe a mechanism of nonlinearity of the light–current characteristic common to heterostructure lasers with a reduced-dimensionality active region. It arises from (i) noninstantaneous carrier capture into the active region and (ii) nonlinear (in the carrier density) recombination rate outside the active region. Because of (i), the carrier density outside the active region rises with injection current above threshold, and because of (ii), the useful fraction of current (that ends up as output light) decreases. We derive a universal closed-form expression for the internal differential quantum efficiency that holds true for quantum well, quantum wire, and quantum dot lasers. © 2002 American Institute of Physics. [DOI: 10.1063/1.1508171]

Reducing dimensionality of the active region significantly improves the performance of semiconductor lasers.¹ Quantum well (QW) lasers have replaced bulk lasers in commercial applications.² Further enhancement is expected for lasers with lower dimensionality, such as quantum wire (QWR) and especially quantum dot (QD) lasers.^{1–4}

In all reported QW, QWR, and QD laser structures, the quantum-confined active elements are embedded in a bulk reservoir region [which also serves as an optical confinement layer (OCL)] wherefrom carriers are fed via some sort of a capture process. Since the capture process is never instantaneous, it gives rise to a current dependence of the carrier density in the reservoir n , even above threshold when the carrier density in the active region itself is pinned by the steady-state generation condition. The increasing n leads to an increase in the parasitic current corresponding to carrier recombination in the reservoir, and contributes to a deviation of the internal differential quantum efficiency η_{int} from unity. This fact was noted earlier^{5–9} but the actual reduction in η_{int} has never been quantified.

In this letter, neglecting other known mechanisms of nonlinearity (such as lattice and carrier heating), we show that the “reservoir effect,” combined with the nonlinear (superlinear in n) dependence of the recombination rate in the reservoir, gives a major contribution to the sublinearity of the light–current characteristic (LCC) at high injection currents—comparable in magnitude to the entire experimentally observed LCC degradation. This suggests that the reservoir effect is a dominant mechanism limiting both the output power and the linearity of the LCC.

The steady-state rate equations for the carriers confined

in the active region and the free carriers in the OCL can be written as follows:

$$j_{\text{capt}} - j_{\text{esc}} - j_{\text{spon}}^{\text{active}} - j_{\text{stim}} = 0, \quad (1)$$

$$j_{\text{esc}} - j_{\text{capt}} - j^{\text{OCL}} + j = 0, \quad (2)$$

where j_{capt} and j_{esc} are, respectively, the current densities of carrier capture into and carrier escape from the active region, $j_{\text{spon}}^{\text{active}}$ and j_{stim} are the spontaneous and the stimulated recombination current densities in the active region, j^{OCL} is the current density of the parasitic recombination in the OCL, and j is the injection current density.

The steady-state rate equation for the photons yields

$$j_{\text{stim}} = e \frac{1}{S} \frac{N}{\tau_{\text{ph}}}, \quad (3)$$

where S is the active layer area (the cross section of the junction), N is the number of photons in the lasing mode, and τ_{ph} is the photon lifetime in the cavity.

The fact that the optical gain g pins above threshold and hence so does the carrier density in the active region, immediately follows from Eq. (3), taking into account that $j_{\text{stim}} \propto gN$.

Since j_{esc} and $j_{\text{spon}}^{\text{active}}$ are both controlled by the carrier density in the active region, they also clamp above threshold. On the other hand, the capture current is linearly related to the carrier density n in the OCL, $j_{\text{capt}} = e v_{\text{capt}} n$, where v_{capt} is the capture velocity (in cm/s). Thus, we obtain from Eq. (1)

$$n = n_{\text{th}} \left(1 + \frac{j_{\text{stim}}}{j_{\text{capt,th}}} \right), \quad (4)$$

where n_{th} and $j_{\text{capt,th}}$ are the threshold values of n and j_{capt} , respectively. The slower the carrier supply to the active region (the lower $j_{\text{capt,th}}$), the larger is $n - n_{\text{th}}$.

^{a)}Electronic mail: asryan@ece.sunysb.edu

^{b)}Electronic mail: Serge.Luryi@sunysb.edu

^{c)}Electronic mail: suris@theory.ioffe.rssi.ru

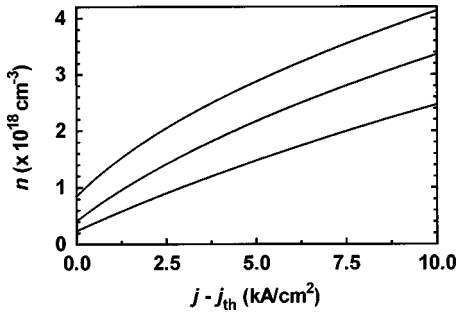


FIG. 1. Injection current density dependence of the free carrier density n in the OCL reservoir for different ratios $j_{\text{th}}^{\text{OCL}}/j_{\text{capt,th}}$, as illustrated by exemplary calculations specific to QD lasers. The variation of $j_{\text{th}}^{\text{OCL}}/j_{\text{capt,th}}$ and j_{th} is accomplished by changing the surface density N_S of QDs. The values of $j_{\text{th}}^{\text{OCL}}/j_{\text{capt,th}}$ for the different curves (from bottom to top) are 0.033, 0.115, and 0.523; the j_{th} values are 31.54, 83.85, and 336.99 A/cm²; they correspond to N_S values of $4\times$, $3.3\times$, and 2.9×10^{10} cm⁻², respectively. Room-temperature operation near 1.55 μm for a GaInAsP/InP heterostructure (see Refs. 10 and 11) is considered. The capture cross section into a QD is plausibly taken to be 10^{-13} cm² (see Ref. 11). We assume 10% QD size fluctuations. The facet reflectivities, the cavity length, and the lateral size are $R=0.32$, $L=1$ mm, and $W=2$ μm .

With Eqs. (1) and (2) and taking into account that $j_{\text{spon}}^{\text{active}}$ pins above threshold, the excess injection current density $j - j_{\text{th}}$ is

$$j - j_{\text{th}} = j_{\text{th}}^{\text{OCL}} - j_{\text{th}}^{\text{OCL}} + j_{\text{stim}}, \quad (5)$$

where $j_{\text{th}} = j_{\text{th}}^{\text{OCL}} + j_{\text{spon}}^{\text{active}}$ is the threshold current density, with $j_{\text{th}}^{\text{OCL}}$ being the value of $j_{\text{th}}^{\text{OCL}}$ at $n = n_{\text{th}}$.

When the dominant recombination channel in the OCL is spontaneous radiation, then $j_{\text{th}}^{\text{OCL}} \propto n^2$ [with n given by Eq. (4)]. Using this in Eq. (5) yields

$$\frac{j - j_{\text{th}}}{j_{\text{th}}^{\text{OCL}}} = \left(1 + \frac{j_{\text{stim}}}{j_{\text{capt,th}}}\right)^2 - 1 + \frac{j_{\text{stim}}}{j_{\text{th}}^{\text{OCL}}}. \quad (6)$$

The solution of the quadratic Eq. (6) gives j_{stim} as a function of $j - j_{\text{th}}$; substituting this function into Eq. (4), we obtain an expression for n (Fig. 1).

The internal differential quantum efficiency of a semiconductor laser is defined as the fraction of the excess injection current that results in stimulated emission: $\eta_{\text{int}} = j_{\text{stim}}/(j - j_{\text{th}})$. With j_{stim} from Eq. (6), we find

$$\eta_{\text{int}} = \frac{1}{\frac{1}{2} + \frac{j_{\text{th}}^{\text{OCL}}}{j_{\text{capt,th}}} + \sqrt{\left(\frac{1}{2} + \frac{j_{\text{th}}^{\text{OCL}}}{j_{\text{capt,th}}}\right)^2 + \frac{j_{\text{th}}^{\text{OCL}}}{j_{\text{capt,th}}} \frac{j - j_{\text{th}}}{j_{\text{capt,th}}}}. \quad (7)$$

We see that η_{int} is a decreasing function of $j - j_{\text{th}}$ (Fig. 2). The output optical power is of the form $P = (\hbar\omega/e)S(j - j_{\text{th}})\eta_{\text{int}}\beta/(\beta + \alpha_{\text{int}})$ where $\hbar\omega$ is the photon energy, and β and α_{int} are the mirror and internal losses, respectively. Thus, the output power is sublinear in the injection current (Fig. 3). This mechanism of nonlinearity is inherent to quantum-confined lasers of arbitrary dimensionality.

For a given $j - j_{\text{th}}$, the internal quantum efficiency and the output power are controlled by the dimensionless parameter $j_{\text{th}}^{\text{OCL}}/j_{\text{capt,th}}$, which is the ratio of the recombination current in the reservoir to carrier capture current, both taken at threshold. Lowering this ratio will make η_{int} closer to unity (Fig. 2) and the LCC more linear (Fig. 3). Ideally, when this

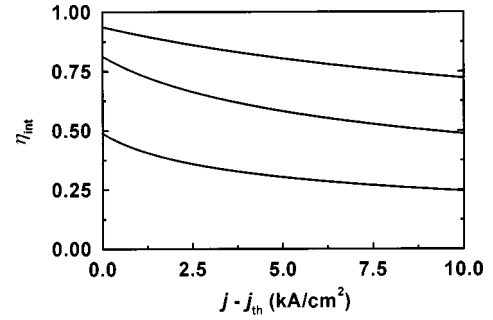


FIG. 2. Internal quantum efficiency against excess injection current density for different ratios $j_{\text{th}}^{\text{OCL}}/j_{\text{capt,th}}$. The values of $j_{\text{th}}^{\text{OCL}}/j_{\text{capt,th}}$, j_{th} , and N_S (from the top down) are the same as in Fig. 1.

ratio vanishes (e.g., when $j_{\text{th}}^{\text{OCL}}=0$ —no recombination in the OCL), $\eta_{\text{int}}=1$ at an arbitrary injection current and the LCC is linear. In general, however, $j_{\text{th}}^{\text{OCL}}$ is a tangible fraction of the total j_{th} , and $\eta_{\text{int}} < 1$ even at $j = j_{\text{th}}$. It is this component that should, first of all, be suppressed to minimize j_{th} and optimize the structure.¹⁰ The conclusion that high power performance of a laser is inseparably controlled by the threshold characteristics is of great importance. The higher the excess of the injection current over the threshold current, the stronger this relation is manifested (Figs. 2 and 3). The higher is the required output power, the lower should be j_{th} (Fig. 3). Since QD lasers offer the lowest j_{th} , our results prove there another—extremely important—potential advantage, namely the possibility of achieving the highest output powers.

At high injection currents, we have

$$\eta_{\text{int}} = \frac{j_{\text{capt,th}}}{\sqrt{j_{\text{th}}^{\text{OCL}}(j - j_{\text{th}})}} \quad (8)$$

$$n = n_{\text{th}} \sqrt{\frac{j - j_{\text{th}}}{j_{\text{th}}^{\text{OCL}}}} \quad (9)$$

$$P = \frac{\hbar\omega}{e} S j_{\text{capt,th}} \sqrt{\frac{j - j_{\text{th}}}{j_{\text{th}}^{\text{OCL}}}} \frac{\beta}{\beta + \alpha_{\text{int}}}. \quad (10)$$

Thus, in the limit of high injection currents, the LCC is strongly sublinear (Fig. 3); n and P increase as $\sqrt{j - j_{\text{th}}}$ (Figs. 1 and 3), while η_{int} decreases as $1/\sqrt{j - j_{\text{th}}}$ (Fig. 2); $\eta_{\text{int}} \ll 1$

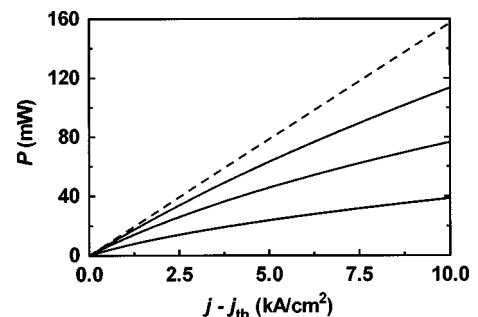


FIG. 3. LCC for different ratios $j_{\text{th}}^{\text{OCL}}/j_{\text{capt,th}}$. The dashed line corresponds to the ideal situation, $j_{\text{th}}^{\text{OCL}}/j_{\text{capt,th}}=0$ ($\eta_{\text{int}}=1$). The values of $j_{\text{th}}^{\text{OCL}}/j_{\text{capt,th}}$, j_{th} , and N_S (from the top down) are the same as in Fig. 1. We disregard free-carrier absorption in the OCL (see Refs. 6 and 7) by putting the internal loss $\alpha_{\text{int}}=0$.

and $n \gg n_{th}$. These square root dependences result from the assumed bimolecular ($\propto n^2$) recombination in the OCL.

The higher the degree of superlinearity of the recombination rate in the OCL with respect to n , the higher the degree of sublinearity of the LCC. Since the nonradiative Auger recombination rate in the OCL increases as n^3 , this recombination channel can become dominant with increasing injection current. In this limit, the difference $j^{OCL} - j_{th}^{OCL}$ in Eq. (5) will be dominated by the cubic (in j_{stim}) term, i.e., $j - j_{th} \propto j_{stim}^3$. Hence, both j_{stim} and P will be proportional to $\sqrt[3]{j - j_{th}}$ and $\eta_{int} = j_{stim} / (j - j_{th}) \propto j_{stim} / j_{stim}^3 = 1/j_{stim}^2 \propto 1/(j - j_{th})^{2/3}$.

The higher the excess current $j - j_{th}$, the larger fraction of it goes into parasitic recombination (first spontaneous and then Auger) outside the active region.

As seen from Eqs. (8) and (10), at high injection currents, the laser performance is controlled by the carrier capture into the active region. To accommodate carrier consumption by the active region, carriers accumulate in the OCL much in excess of their threshold amount. The resultant superlinear increase in parasitic recombination degrades the LCC. In this context, we note a radical design strategy, recently proposed to improve the temperature stability of QD lasers.^{12,13} In this approach, the two reservoirs feeding carriers into the quantum-confined region are essentially unipolar and the finite-delay capture process is not accompanied by a buildup of a bipolar carrier density and additional recombination. We therefore expect that lasers designed according to Refs. 12 and 13 will exhibit linear behavior and excellent power performance.

In conclusion, we have identified a type of sublinearity of the LCC of semiconductor lasers with a quantum-confined

active region and derived a universal expression for the current dependence of their internal differential quantum efficiency η_{int} . This expression retains the same form for QD, QWR, and QW lasers.

The actual shape of nonlinear LCC depends on the dominant recombination channel outside the active region. Analysis of the LCC shape provides, therefore, a method for identifying the dominant recombination channel in the OCL.

We demonstrate a direct relationship between the power and threshold characteristics in the sense that reducing j_{th} is a key to increasing η_{int} and P . This indicates that for high power applications, QD lasers may have a major advantage over conventional QW lasers.

¹R. Dingle and C. H. Henry, US Patent No. 3,982,207 (Sept. 21, 1976).

²*Quantum Well Lasers*, edited by P. S. Zory, Jr. (Academic, Boston, 1993), p. 504.

³Y. Arakawa and H. Sakaki, Appl. Phys. Lett. **40**, 939 (1982).

⁴N. N. Ledentsov, M. Grundmann, F. Heinrichsdorff, D. Bimberg, V. M. Ustinov, A. E. Zhukov, M. V. Maximov, Z. I. Alferov, and J. A. Lott, IEEE J. Sel. Top. Quantum Electron. **6**, 439 (2000).

⁵N. Tessler, R. Nagar, G. Eisenstein, S. Chandrasekhar, C. H. Joyner, A. G. Dentai, U. Koren, and G. Raybon, Appl. Phys. Lett. **61**, 2383 (1992).

⁶H. Hirayama, J. Yoshida, Y. Miyake, and M. Asada, Appl. Phys. Lett. **61**, 2398 (1992).

⁷H. Hirayama, J. Yoshida, Y. Miyake, and M. Asada, IEEE J. Quantum Electron. **30**, 54 (1994).

⁸L. A. Coldren and S. W. Corzine, *Diode Lasers and Photonic Integrated Circuits* (Wiley, New York, 1995), p. 594.

⁹P. M. Snowton and P. Blood, IEEE J. Sel. Top. Quantum Electron. **3**, 491 (1997).

¹⁰L. V. Asryan and R. A. Suris, Semicond. Sci. Technol. **11**, 554 (1996).

¹¹L. V. Asryan and R. A. Suris, IEEE J. Quantum Electron. **36**, 1151 (2000).

¹²L. V. Asryan and S. Luryi, IEEE J. Quantum Electron. **37**, 905 (2001).

¹³L. V. Asryan and S. Luryi, Solid-State Electron. **46**, (2002) (in press).